EMBEDDING TECHNIQUES OF FBG SENSORS IN ADHESIVE LAYERS OF COMPOSITE STRUCTURES AND APPLICATIONS

S. Kim[1], S. Yoo[1], E. Kim[1], I. Lee[1]*, I. Kwon[2], D. Yoon[2]
[1] School of Mechanical, Aerospace and Systems Engineering, KAIST, Daejeon, S. Korea,
[2] Center for Safety Measurement, KRISS, Daejeon, S. Korea.
* Corresponding author (inlee@kaist.ac.kr)

Keywords: *FBG sensor, embedding technique, peak split, composite structure, debonding, SHM*

1 Introduction

Recently, adhesive bonding is widely used for the connection of composite structures. However, the more use of adhesive bonding method rise, the more frequency of adhesive failure increase.

Several researchers have studied adhesive monitoring using optical fiber sensors such as fiber Bragg grating (FBG) sensors, but they focused on the limited applications such as composite repair patches [1-4] with thin adhesive layer and a small number of voids. That is, few studies have been reported on the adhesive monitoring in thick adhesive layer with a number of voids.

Embedded FBG sensors in adhesive layer are efficient and favorable for adhesive monitoring. However, severe problems including peak splits, bandwidth changes, and others can occur during the embedding process of FBG sensors.

Kang *et al.* [5] showed that split problems can be reduced by shortening the grating length when the FBG sensors are embedded into the composite specimens. In this study, three embedding techniques are suggested to prevent the unexpected problems when FBG sensors are embedded into adhesive layers. The signal characteristics of the reflected spectra of FBG sensors for each technique are quantitatively investigated, and the most effective method is recommended.

Moreover, the embedding technique applied specimens are designed and fabricated. Three point bending tests are carried out for demonstrating the feasibility of embedding technique for adhesive monitoring.

2 Embedding Techniques

2.1 Classification of Specimens

Three techniques were suggested when the FBG sensors are embedded into the adhesive layer: a) pre-attachment and curing (PAC) technique, b) recoating technique, c) packaging technique. For PAC technique, the FBG sensors are protected by the pre-attachment process. Recoating technique is the reinforcement method that the UV acrylate protects weak Bragg grating element. Packaging technique is also one of the reinforcement skill that epoxy adhesive protects weak elements.

The classification of specimens for embedding techniques is shown in Table 1. The eight kinds of specimens were manufactured. The bare FBG sensors applied specimens (B0 and B1) were fabricated as comparison group. In this study, the effects of voids were considered since unexpected voids can produce birefringence and internal strain gradients in Bragg grating elements during curing. Thus, artificial voids were applied to the specimen Pr1, R1, P1, and B1 to assess the effect of voids, while the others (Pr0, R0, P0 and B0) have no artificial voids. All specimens have two FBG sensors to reduce experimental errors.

2.2 Fabrication of specimens

The specimens were made of epoxy adhesive (KFR-730F with KFH-730F/ KUKDO Chemical Co., Ltd.), composites (Unidirectional E-glass reinforced composite/ Owens corning Ltd.), cork, and two FBG sensors. The thickness of bonding line of wind turbine blades (6 *mm* or less [6]), was considered to determine the thickness of adhesive layer of specimen (4 *mm*). The corks were used for protecting the fibers, and maintaining the thickness of adhesive layer during curing.

The specimens were fabricated by following procedure depending on each techniques. PAC technique has simple manufacturing processes: a)

FBG sensors are aligned, b) the sensors are covered with first adhesive, c) it is cured under the specific conditions (which depends on a kind of adhesive/ 80 ℃ for 24 *hrs*), d) adhesive layer is constructed, e) composite component is assembled, and f) this is cured under the same condition of c). Figure 1 shows the fabrication steps of specimen Pr0. The fabricating procedure of recoating technique applied specimens is similar to those of PAC applied specimen, but the pre-attachment and curing process were omitted. Packaging technique applied specimens were fabricated through same procedure of recoating applied specimens, but the packaged FBG sensors were used instead of recoated FBG sensors. The packaging material is identical to adhesive layer of specimen. Figure 2 presents the packaged FBG sensors.
Artificial voids were applied to the four specimens (Pr1, R1, P1 and B1) by using a syringe as shown in Figure 3.

2.3 Experiment

The reflected peak signals of the FBG sensors were traced at each step of the embedding techniques by interrogator, CyT-FMI-3-100. For examples, the specimen pr0 and pr1 have five steps for data acquisition: i) before installation of FBG sensors, ii) after 1st adhesive, iii) after pre-curing, iv) after 2nd adhesive, v) after curing. The others have three steps: i) before embedding of FBG sensors, ii) after embedding, iii) after curing.

2.4 Results and Discussion

The signal comparison tests were carried out. From Figure 4 to Figure 7 show the wavelength changes of the specimens during the process of embedding techniques.

2.4.1 Peak Signal Changes
Multi-peaks did not occur, when artificial voids were not applied. The specimens (Pr0, R0, P0, and B0) without artificial voids showed clearly sharp peak during whole processes. However, some of specimens showed significant signal changes depending on the applied techniques, when artificial voids were applied. The specimen Pr1 and R1 did not show the peak splits, while the specimen P1 and B1 showed the multi-peaks induced by birefringence and internal strain gradients during curing process. These results indicate that the FBG sensors were protected against non-uniform residual strain. For specimen P1, the epoxy adhesive packaged sensors were affected by non-uniform stresses when adhesive near the artificial voids were contracted. These showed that the packaged FBG sensor could not prevent internal strain gradients during curing. Moreover, the specimen B1 also showed similar tendencies to the specimen P1. The peak splits can cause strain measurement errors, and thus it is imperative that the special techniques are applied when FBG sensors are embedded into adhesive layer.

2.4.2 3-dB Bandwidth Changes
The 50% reflectivity of reflected peak signals, full width half maximum (FWHM) value, was investigated to observe the bandwidth changes of FBG sensors. The changes of FWHM values at each step of embedding techniques are illustrated in Figure 4 – Figure 7, and the final values of FWHM are presented in Table 2. The bandwidth changes showed less than 50% for the specimens (Pr0, R0, P0, and B0) without artificial voids, while the specimens (Pr1, R1, P1, and B1) with artificial voids were depending on the applied techniques. The 3-*dB* bandwidth change of the specimen Pr1 became only 0.33 and 0.5 times changed for the sensor 1 and 2, respectively. For the specimen R1, the FWHM value of the sensor 1 and 2 became 50% broader. Of particular interest is that the specimen P1 and B1 showed significant changes of FWHM values. The specimen P1 presented the bandwidth change of 200% for the sensor 1 and 133% change for the sensor 2. For the specimen B1, the bandwidth values became 2 times broader. Thus, the PAC technique or recoating technique applied specimens produced relatively small changes of FWHM values compared to the packaging technique or bare FBG sensor applied specimens.
In this study, PAC technique was determined to apply for embedding, since it was simple, and could effectively prevent split problems.

3 Debonding monitoring

Simple specimens which replicate the load and structural conditions of wind turbine blades were

designed as shown in Figure 8. Two specimens were fabricated considering the debonding effects: i) the specimens with artificial debonding (Figure 8), ii) the specimen without artificial debonding. Artificial debonding was applied to the specimen using release agent (Frekote 770-NC/ Henkel Corp.), and partially bonded area exists within the debonding region as shown in Figure 8. It can simulate the perfect debonding of adhesive layer during operation. Same materials used in the experiment of peak signal changes were used. Two multiplexed FBG sensors were embedded into the adhesive layer (1 *mm* apart from the interface between adhesive layer and composite) of the specimens through PAC technique. Three point bending tests (1st point: 15 *mm* apart from the left side edges, 2nd point: center, 3rd point: 15 *mm* apart from the right side edge) were carried out using UTM, INSTRON 4428 with a displacement control of 2.0 *mm/min* at room temperature.

It was observed that the initial peak signals from the FBG sensors with PAC technique did not present peak splits, after fabricating the specimens. The strain changes of specimen according to load are shown in Figure 9. Debonding was observed at 447 *N* by FBG sensor 1 of the specimen with artificial debonding. The strain measured by FBG sensor 1 sharply increased due to debonding, after then large fluctuations appeared. These results indicate that unexpected debonding can be easily founded by comparing the strain changes.

Thus, PAC technique has proved the feasibility for the applications of sensor embedding as well as debonding monitoring.

4 Conclusions

Three embedding techniques were suggested to prevent split problems. The signals characteristics of FBG sensors for each technique were compared. PAC technique showed a great ability to prevent split problems, relatively small bandwidth changes, and others. Moreover, it was experimentally verified that PAC technique has the sufficient feasibility for the applications of debonding monitoring. Therefore, we can conclude that PAC technique is considered as the most effective method for the embedding of FBG sensors among the suggested embedding techniques.

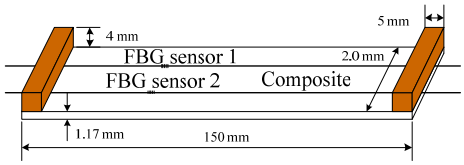

(a) Installation of two FBG sensors

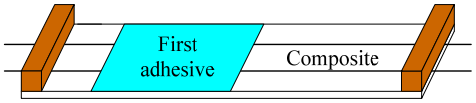

(b)~(c) Pre-attachment and curing process

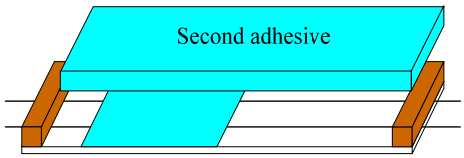

(d) Construction of adhesive layer

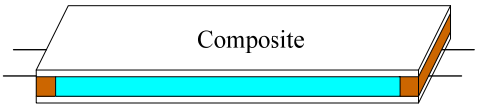

(e)~(f) Curing and assembling process

Fig.1. Fabricating procedure of specimen Pr0

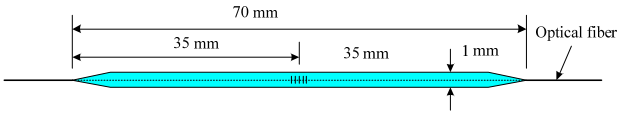

(a) Schematic of packaged FBG sensor

(b) Fabricated FBG sensor

Fig.2. Photo of packaged FBG sensors

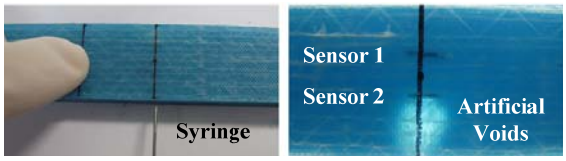

Fig.3. Application of artificial voids

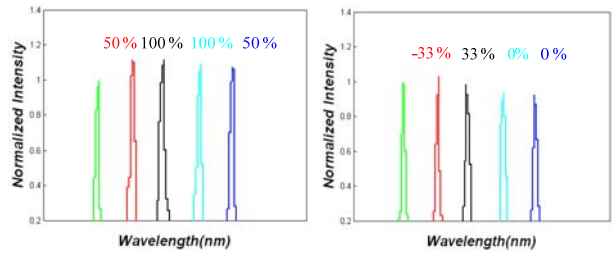

(a) Specimen Pr0 (left: sensor1, right: sensor2)

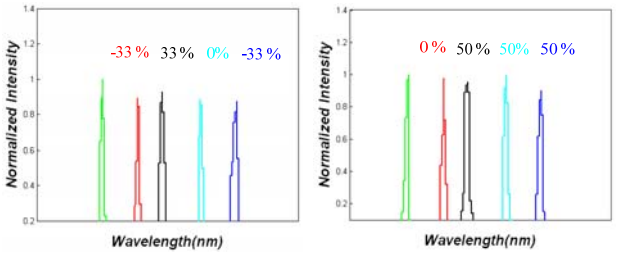

(b) Specimen Pr1 (left: sensor1, right: sensor2)

Fig.4. Wavelength changes of specimen Pr0 and Pr1

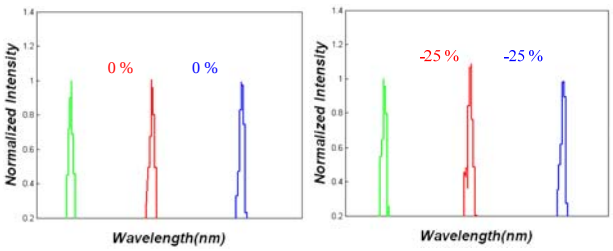

(a) Specimen P0 (left: sensor1, right: sensor2)

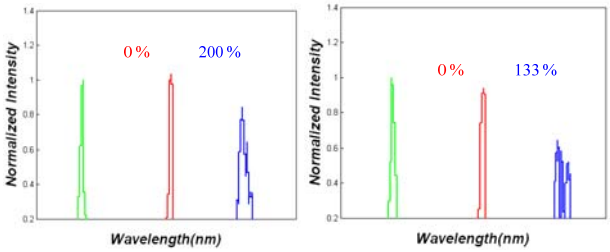

(b) Specimen P1 (left: sensor1, right: sensor2)

Fig.6. Wavelength changes of specimen P0 and P1

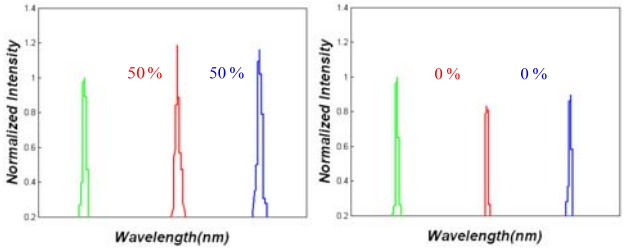

(a) Specimen R0 (left: sensor1, right: sensor2)

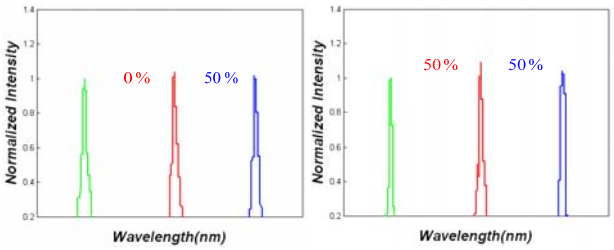

(b) Specimen R1 (left: sensor1, right: sensor2)

Fig.5. Wavelength changes of specimen R0 and R1

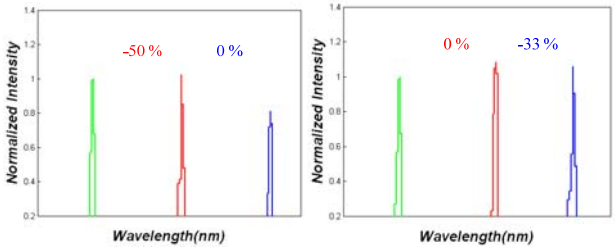

(a) Specimen B0 (left: sensor1, right: sensor2)

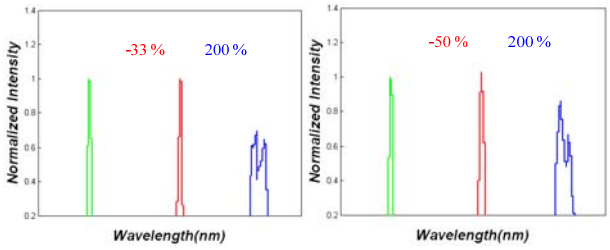

(b) Specimen B1 (left: sensor1, right: sensor2)

Fig.7. Wavelength changes of specimen B0 and B1

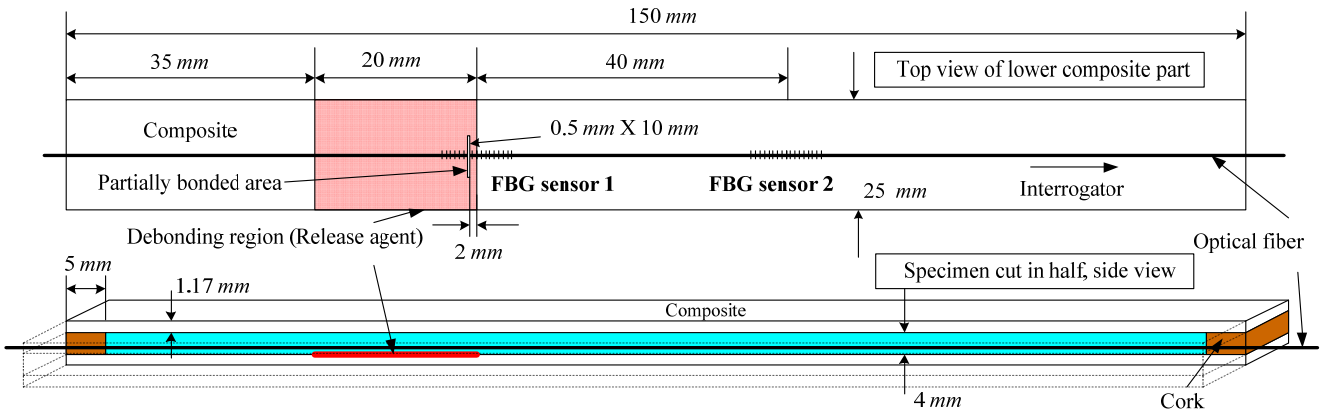

Fig.8. Designed specimen with PAC technique

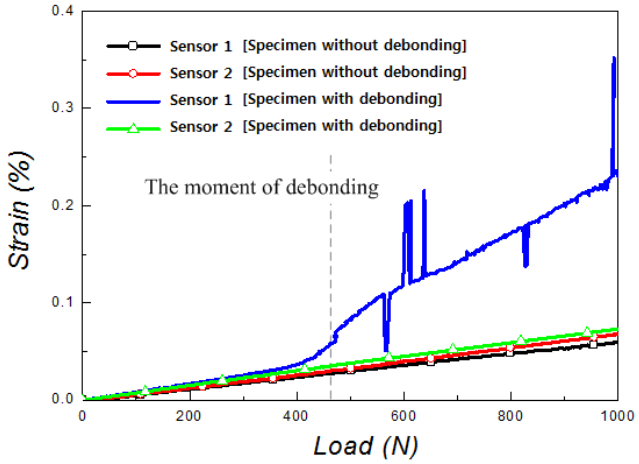

Fig.9. Strain change of FBG sensors

Specimen no.	Specimen	
	Technique	Initial peak wavelength (Sensor1 / Sensor2)
Pr0	PAC	1553.1 *nm* / 1553.0 *nm*
Pr1		1552.8 *nm* / 1553.4 *nm*
R0	Recoating	1551.6 *nm* / 1551.5 *nm*
R1		1551.5 *nm* / 1551.7 *nm*
P0	Packaging	1552.0 *nm* / 1552.2 *nm*
P1		1555.6 *nm* / 1557.0 *nm*
B0	Bare FBG	1553.2 *nm* / 1553.2 *nm*
B1		1553.0*nm* / 1552.9 *nm*

Table.1. Classification of specimens

Specimen no.	Bandwidth change (%)	
	Sensor 1	Sensor 2
Pr0	50	0
R0	50	0
P0	0	-25
B0	0	-33
Pr1	-33	50
R1	50	50
P1	**200**	**133**
B1	**200**	**200**

Table.2. 3-*dB* bandwidth changes of specimens

Acknowledgement

This research was supported by New & Renewable Energy R&D program under the Korea Ministry of Knowledge Economy (2008-N-WD08-P-01), by WCU (World Class University) program through the National Research Foundation of Korea funded by the Ministry of Education, Science and Technology (R31-2008-000-10045-0), and by the third stage of the Brain Korea 21 Project in 2011. Authors are grateful for their supports.

References

[1] S. Takeda, T. Yamamoto, Y. Okabe and N. Takeda, “Debonding monitoring of composite repair patches using embedded small-diameter FBG sensors”, *Smart Materials and Structures*, Vol.16, No. 3, pp.763-770, 2007.6.

[2] R. Hones and S. Galea, “Health monitoring of composite repairs and joints using optical fibre”, *Composite Structures*, Vol.58, No.3, pp.397-403. 2002. 11.

[3] Shu Minakuchi, Yoji Okabe and Nobuo Takeda, “ Real-time Detection of Debonding between Honeycomb Core and Facesheet using a Small-diameter FBG Sensor Embedded in Adhesive Layer”, Journal of Sandwich Structures and Materials, Vol. 9, No. 1, pp.9-33, 2007

[4] J. Palaniappan, S.L. Ogin, A.M. Thorne, G.T. Reed, A.D. Crocombe, T.F. Capell, S.C. Tjin, L. Mohanty, “ Disbond growth detection in composite–composite single-lap joints using chirped FBG sensors.”, Composites Science and Technology, Vol. 68, No. 12, pp. 2410-2417, 2008.

[5] D.H. Kang, S.O. Park, C.S. Hong and C.G. Kim, “The signal characteristics of reflected spectra of fiber Bragg grating sensors with strain gradients and grating length”, *NDT&E International*, Vol. 38, No.8, pp.712-718, 2005.12.

[6] Kyle K. Wetzel, “Defect-Tolerant Structure Design of Wind Turbine Blades”, 50th AIAA/ ASME/ ASCE/ AHS/ ASC Structures, Structural Dynamics, and Materials Conference, Palm Spring, California, 2009.5.